Supporting Information

Pecqueur et al. 10.1073/pnas.1204129109

SI Methods

Ribosome Display Selection and Binder Identification. All selection steps were carried out at 4 °C. Decreasing concentrations of tubulin (250, 100, 20, and 10 nM) were used in successive rounds of selection. After in vitro translation, the designed ankyrin repeat protein (DARPin) library was incubated with the target for 30 min and washed six times with 20 mM Pipes, pH 6.8, 150 mM KCl, 50 mM Mg-Acetate, 0.05% Tween-20, and 0.1 mM GTP (buffer WBT). Total wash times were increased from 7 to 40 to 60 min in successive rounds. From the second round onward, the translation mix containing the ternary mRNA–ribosome–DARPin complexes was first prepanned for 15 min in a well without the biotinylated target. In the third round, an additional "off-rate" selection step (1) was performed by washing for 30 min with 2 μM tubulin in 100 μL WBT. RNA from selected binders was eluted with 50 mM Tris acetate, pH 7.6 (4 °C), 100 mM NaCl, and 25 mM EDTA (200 μL) and reverse transcribed to cDNA. Following this, the cDNA was amplified by 40, 30, 28, and finally 25 PCR cycles in the successive rounds.

To screen single clones, MaxiSorp plates (Nunc) were coated with neutravidin in TBS [50 mM Tris pH 7.4 (4 °C), 150 mM NaCl] and then blocked with 0.2% BSA in TBS supplemented with 0.05% Tween-20 (TBST) for 1 h at room temperature. They were incubated with biotinylated peptide-coupled tubulin (15 nM) in 100 μL PBST (20 mM Pipes, pH 6.8, 1 mM Mg-acetate, 150 mM KCl, 0.05% Tween) for 30 min at 4 °C. After washing, 5 μL of cell lysate was mixed with 95 μL of PBST supplemented with 0.2% BSA and added to the target-containing wells or to a control without immobilized tubulin. After a 1-h incubation at 4 °C, wells were washed with PBST and a 1:5,000 dilution of an anti-RGS$(H)_4$ antibody (Qiagen) was added and incubated for 1 h at 4 °C. After a washing step, a 1:10,000 dilution of a goat anti-mouse IgG-AP-conjugate antibody (Pierce) was added (1 h, 4 °C). Binding was detected by monitoring the absorbance at 405 nm due to the hydrolysis of disodium 4-nitrophenyl phosphate (Fluka) catalyzed by alkaline phosphatase in 50 mM $NaHCO_3$, 50 mM $MgCl_2$. The amino acid sequences of the selected DARPins were obtained by DNA sequencing.

Protein Purification and Labeling. Sheep brain tubulin was purified by two polymerization/depolymerization cycles in a high-molarity buffer (2) and stored in liquid N_2 in 50 mM Mes-K, pH 6.8, 33% (vol/vol) glycerol, 0.25 mM $MgCl_2$, 0.5 mM EGTA, and 0.1 mM GTP until use. Before use, an additional microtubule assembly/disassembly cycle was performed to remove any nonfunctional protein. The disassembly step was carried out in 15 mM Mes-K, pH 6.8, 0.5 mM $MgCl_2$, and 0.5 mM EGTA. Tubulin concentration was determined spectrophotometrically using an extinction coefficient at 278 nm of 1.2 $mg^{-1}{\cdot}mL^{-1}{\cdot}cm^{-1}$ assuming the molecular mass of the heterodimer is 100 kDa (3).

The D1 DARPin was expressed in XL1-Blue cells grown in 2YT medium. When A_{600} reached 0.7–0.8, protein expression was induced with 0.5 mM isopropyl β-D-1-thiogalactopyranoside for 4 h at 37 °C. Cells were resuspended in 10 mL/g of wet cells of 50 mM Tris, pH 8 (4 °C), 1 mM $MgCl_2$, 10 mM imidazole, 0.3 mg/mL lysozyme, and protease inhibitor mix (complete EDTA free; Roche Applied Science). Cells were lysed by sonication and cell debris was removed by centrifugation at 20,000 × *g* for 20 min at 4 °C. Purification was performed on a Äkta Purifier system using Histrap columns (GE Healthcare). Eluted protein was subjected to size exclusion chromatography on a Superdex 75 column equilibrated with 20 mM potassium phosphate, pH 7.2, 1 mM $MgCl_2$, 0.5 mM EGTA, and 100 mM KCl (buffer A). D1 concentration was estimated by UV absorption, using an extinction coefficient of 6,990 $M^{-1}{\cdot}cm^{-1}$ derived from the peptide sequence using the ProtParam webserver (http://web.expasy.org/protparam).

For labeling with a fluorescent probe, the D160C mutation was introduced using the QuikChange strategy and the following primers: 5′-CCATCGACAACGGTAACGAGTGCCTGGCTGAAATCCTGC-3′ (forward) and 5′-GCAGGATTTCA GCCAGGCACTCGTTACCGTTGTCGATGG-3′ (reverse). PCR was performed with Pfu polymerase (ThermoScientific).

Oregon Green 488 maleimide was purchased from Life Technologies. D1-D160C (0.1 mM) was reduced with 2 mM DTT for 30 min at room temperature. DTT was removed on a Bio-Gel P-6 (Micro Bio-Spin 6; Bio-Rad). Then a 7.5-fold molar excess of dye dissolved at 15 mM in DMSO was added dropwise. The reaction was performed in buffer A for 1 h at 25 °C and then for 2 h at 4 °C. Excess dye was inactivated by addition of 2 mM β-mercaptoethanol. Unreacted dye was removed using a Bio-Gel P-6 followed by two 2-h dialyses in 200 mL of buffer A at 4 °C or by size-exclusion chromatography on a Superdex 200 10/300 GL (GE Healthcare). The degree of labeling was estimated according to standard procedures (Invitrogen) from the relative absorbance at 280 nm and at 494 nm, using an extinction coefficient of 68,000 $M^{-1}{\cdot}cm^{-1}$ for Oregon Green (4). Protein concentration was confirmed by a BCA assay (Pierce), using RB3-SLD quantified by amino acid content analysis following complete acid hydrolysis as a standard. Data were corrected for the number of amide bonds in the reference and the test sample. Tubulin was labeled with Alexa568 (Invitrogen), Cy5 (Lumiprobe), or biotin (Pierce) as described in ref. 5.

$(D1)_2$ was generated by inserting the flexible linker $(Gly_4Ser)_3$ between monomers. The gene encoding $(D1)_2$ was assembled in a derivative of the vector pQE30 with the additional gene *lacI* allowing the construction of tandem DARPins with N-terminal MRGS$(H)_6$ tag and spaced by a $(GGGGS)_3$ linker. $(D1)_2$ was expressed in *Escherichia coli* BL21 DE3 and the product was purified as described above. $(D1)_2$ concentration was estimated by UV absorption, using an extinction coefficient of 13,980 $M^{-1}{\cdot}cm^{-1}$ derived from the peptide sequence using the ProtParam webserver.

GFP-$CLIP_{MTB}$ from *Homo sapiens*, kinesin 14 from *Xenopus laevis* (XCTK2), and Mal3-GFP from *Schizosaccharomyces pombe* were purified as described in refs. 6–8.

Fluorescence Anisotropy. Dissociation constant determination was performed in buffer A at 20 °C by titrating 120 nM of D1-D160C–Oregon Green 488 with increasing amounts of freshly thawed tubulin. Steady-state fluorescence anisotropy was monitored on a Cary Eclipse spectrofluorimeter (Agilent Technologies), using a 496-nm excitation wavelength with a 2.5-nm bandwidth, a 523-nm emission wavelength with a 10-nm bandwidth, and a 1-s integration time. Each titration point was measured 20 times, averaged, and repeated once. Data were fitted to a 1:1 binding isotherm using the quadratic equation

$$r = r_0 + \frac{AB}{A_0}(r_{max} - r_0) \text{ with}$$

$$\frac{AB}{A_0} = \frac{(K_d + A_0 + B_0) - \sqrt{(K_d + A_0 + B_0)^2 - 4A_0}}{2A_0}$$

with A_0 and B_0 corresponding to the initial concentrations of D1 and tubulin, respectively. r is the measured anisotropy, r_0, and r_{max} are the fluorescence anisotropies of D1 and of D1 bound to tubulin.

In Vitro Microtubule Assembly. Concentrations of tubulin ranging from 10 to 45 μM were mixed with 8 or 20 μM D1. Microtubule assembly was monitored turbidimetrically at 340 nm with a Cary 50 spectrophotometer (Agilent Technologies), using a 200-μL, 0.7-cm light path cuvette thermostated at 37 °C until the steady state was reached, and then cooled down to 4 °C to measure the baseline. Experiments were done in 50 mM Mes-K, pH 6.8, 6 mM $MgCl_2$, 30% glycerol, 0.5 mM GTP.

Preparation of the Tubulin-DARPin Complex for Crystallization. Tubulin was incubated at 4 °C for 5 min with a fivefold excess of GTP, following which the C termini of α- and β-tubulin were cleaved with subtilisin (9). D1 was added to digested tubulin in a 1.5:1 ratio. The complex was purified on a Superdex 200 10/300 GL equilibrated in 20 mM Hepes, pH 7.2, 100 mM KCl, 1 mM $MgCl_2$, and 0.5 mM EGTA. Fractions containing the complex were pooled and adjusted to 0.2 mM GTP. Samples were concentrated by ultrafiltration (Vivaspin 500 cutoff 5 kDa; Sartorius) to a 28–35 mg·mL^{-1} concentration, aliquoted, and stored in liquid N_2 until use. Complex concentration was estimated spectrophotometrically, using the sum of the extinction coefficients at 280 nm of tubulin and D1. For crystallization, the protein was diluted to 22–24 mg·mL^{-1}.

Diffraction Data Collection and Structure Determination. A native dataset was collected (100 K, λ = 0.978 Å) from a single Tub-D1 crystal at the SOLEIL beam-line PROXIMA-1 to a resolution of 2.2 Å. Images were processed with XDS (10) and data were scaled with XSCALE (11).

Figures depicting the structural features of tubulin were prepared with PyMOL (http://www.pymol.org). The quality of the final models was checked with MolProbity (12). Interface was analyzed using the protein interfaces, surfaces, and assemblies service PISA (13) at the European Bioinformatics Institute and the protein–protein interaction server ProtorP (14).

Total Internal Reflection Fluorescence (TIRF) Microscopy. ***Measurement of microtubule growth velocity.*** The microtubule growth velocity was measured essentially as described in ref. 15. In brief, biotinylated Alexa568-labeled GMPCPPP-stabilized microtubule seeds are attached to polyethylene glycol (PEG)-biotin–coated glass coverslips via neutravidin (Invitrogen) from which free tubulin dimers (6.5% Alexa568 labeling) polymerize into microtubules. The final imaging buffer (standard TIRF buffer) was 80 mM K Pipes (pH 6.85), 4 mM $MgCl_2$, 1 mM EGTA, 60 mM KCl, 0,1% methylcellulose, 20 mM glucose, 50 μg/mL β-casein, 2 mM GTP, 5 mM 2-mercaptoethanol, 0.66 mg/mL catalase (Sigma), and 1.33 mg/mL glucose oxidase (Serva). The tubulin concentration was 20 μM unless specified otherwise and the DARPin concentration was in the range from 5 nM to 9 μM. Images were recorded at one frame per 3 s (100-ms exposure time) at 30 °C, using an Olympus XI71 TIRF microscope equipped with a 100× oil objective and an Evolve (Photometrics) cooled EM CCD camera.

Microtubule gliding assay. The minus-end–directed motor kinesin 14 (XCTK2) was adsorbed nonspecifically to methoxy-PEG–coated glass (7). Then Alexa568-labeled GMPCPP-stabilized microtubules were allowed to attach to the surface-bound motors. After 3 min at room temperature, unbound GMPCPP microtubules were washed out and replaced by the following solution: 20 μM unlabeled tubulin, 70 nM Mal3-GFP (to visualize growing microtubule ends), and 500 nM unlabeled $(D1)_2$ (or no DARPin for the control experiment) in gliding buffer [40 mM K Pipes (pH 6.85), 8 mM $MgCl_2$, 1 mM EGTA, 30 mM KCl, 0.05% methylcellulose, 20 mM glucose, 250 μg/mL β-casein, 2 mM GTP, 4 mM ATP, 1 mM β-mercaptoethanol, 0.66 mg/mL catalase (Sigma), and 1.33 mg/mL glucose oxidase (Serva)]. Microtubule transport at 30 °C was recorded at one frame per 3 s (100-ms exposure time), using the TIRF microscopy setup as described above. In the presence of $(D1)_2$ all gliding microtubules (40 in two independent experiments) had only their lagging end, i.e., their (−) end, strongly labeled with Mal3-GFP.

Depolymerization protection assay. To determine whether nonstabilized microtubule ends are protected from depolymerization when capped by $(D1)_2$, we first prepolymerized microtubules in a microscopy flow chamber placed on a prewarmed metal block in a temperature-controlled Plexiglas chamber at 30 °C (±1 °C) by elongating them from immobilized Alexa568-labeled GMPCPP-stabilized microtubule seeds in the presence of 15 μM Cy5 (Lumiprobe)-labeled tubulin (labeling ratio of 6.5%) in standard TIRF buffer. After 90 s a new, prewarmed solution was flowed in containing 15 μM unlabeled tubulin, 0.5 μM $(D1)_2$ (or its storage buffer for the control condition), and 65 nM of the GFP-labeled CLIP-170 binding part ($CLIP_{MTB}$, a fragment consisting of amino acids 1–481, previously also called H2) (16) that binds along the entire microtubule under the conditions used here. The flow chamber was transferred to the TIRF microscope and time-lapse imaging started ∼30 s after the final solution was flowed in. Images were recorded for each channel at one frame per 5 s with a 100-ms exposure time. As a measure of microtubule plus-end stability, we quantified how many Cy5-labeled microtubule plus segments (microtubule segments extending from the plus end of the GMPCPP seed) were still present 2 min after introducing the $(D1)_2$-containing solution (or the control solution). Plus and minus segments were discriminated by their growth velocity, which was determined from the analysis of kymographs extracted from the GFP-$CLIP_{MTB}$ signal. Ends growing with more than 1.3 μm·min^{-1} were counted as plus ends. (In the conditions used here, the average growth velocities for plus and minus ends were 1.87 ± 0.35 and 0.63 ± 0.17 μm·min^{-1}, respectively.)

Microtubule growth inhibition in* Xenopus *egg extract. *Xenopus* egg extracts were prepared essentially as described in ref. 17 and supplemented with sperm nuclei and 360 nM Alexa568-labeled tubulin (labeling ratio 53%). After 35–45 min at 18 °C (when astral arrays can be observed) 4 μL were transferred with a cut pipette tip onto a glass coverslip and carefully spread into a thin film of extract without covering it with a coverglass. Asters were allowed to settle for 3 min and the center of the extract film was overlaid with another 5 μL of extract to prevent drying. The sample was then imaged at room temperature by TIRF microscopy (excitation at 488 nm and 561 nm, 100 ms, one frame per 3 s). After ∼90 s, 2 μL of 4.125 μM $(D1)_2$-Alexa488 or GFP in 15 mM sodium phosphate, pH 7.4, 130 mM NaCl, and 100 mM KCl was added to the extract.

1. Zahnd C, Sarkar CA, Plückthun A (2010) Computational analysis of off-rate selection experiments to optimize affinity maturation by directed evolution. *Protein Eng Des Sel* 23:175–184.

2. Castoldi M, Popov AV (2003) Purification of brain tubulin through two cycles of polymerization-depolymerization in a high-molarity buffer. *Protein Expr Purif* 32: 83–88.

3. Correia JJ, Baty LT, Williams RC, Jr. (1987) Mg2+ dependence of guanine nucleotide binding to tubulin. *J Biol Chem* 262:17278–17284.
4. Rusinova E, Tretyachenko-Ladokhina V, Vele OE, Senear DF, Alexander Ross JB (2002) Alexa and Oregon Green dyes as fluorescence anisotropy probes for measuring protein-protein and protein-nucleic acid interactions. *Anal Biochem* 308:18–25.
5. Hyman A, et al. (1991) Preparation of modified tubulins. *Methods Enzymol* 196: 478–485.
6. Bieling P, et al. (2008) CLIP-170 tracks growing microtubule ends by dynamically recognizing composite EB1/tubulin-binding sites. *J Cell Biol* 183:1223–1233.
7. Hentrich C, Surrey T (2010) Microtubule organization by the antagonistic mitotic motors kinesin-5 and kinesin-14. *J Cell Biol* 189:465–480.
8. Maurer SP, Bieling P, Cope J, Hoenger A, Surrey T (2011) GTP-γS microtubules mimic the growing microtubule end structure recognized by end-binding proteins (EBs). *Proc Natl Acad Sci USA* 108:3988–3993.
9. Knipling L, Hwang J, Wolff J (1999) Preparation and properties of pure tubulin S. *Cell Motil Cytoskeleton* 43:63–71.
10. Kabsch W (2010) Xds. *Acta Crystallogr D Biol Crystallogr* 66:125–132.
11. Kabsch W (2010) Integration, scaling, space-group assignment and post-refinement. *Acta Crystallogr D Biol Crystallogr* 66:133–144.
12. Chen VB, et al. (2010) MolProbity: All-atom structure validation for macromolecular crystallography. *Acta Crystallogr D Biol Crystallogr* 66:12–21.
13. Krissinel E, Henrick K (2007) Inference of macromolecular assemblies from crystalline state. *J Mol Biol* 372:774–797.
14. Reynolds C, Damerell D, Jones S (2009) ProtorP: A protein-protein interaction analysis server. *Bioinformatics* 25:413–414.
15. Bieling P, et al. (2007) Reconstitution of a microtubule plus-end tracking system in vitro. *Nature* 450:1100–1105.
16. Scheel J, et al. (1999) Purification and analysis of authentic CLIP-170 and recombinant fragments. *J Biol Chem* 274:25883–25891.
17. Hannak E, Heald R (2006) Investigating mitotic spindle assembly and function in vitro using Xenopus laevis egg extracts. *Nat Protoc* 1:2305–2314.

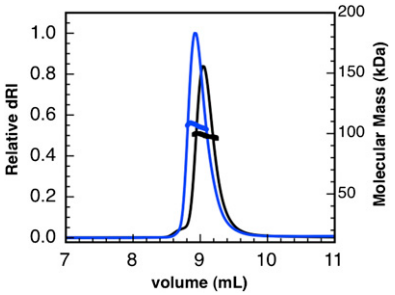

Fig. S1. Size exclusion chromatography coupled to multi-angle light-scattering (SEC-MALLS) analysis of the tubulin–D1 complex. Size exclusion chromatography was carried out on a Prominence HPLC system (Shimadzu), using a KW803 column (Shodex) in 20 mM potassium phosphate, pH 7.2, 1 mM $MgCl_2$, 0.5 mM EGTA, and 100 mM KCl. The variations of differential refractive index (left) and molecular mass (right) are shown. Thirty microliters of a solution of 50 μM tubulin (black) or 50 μM tubulin with a twofold excess of D1 (blue) were loaded on the column running at a flow rate of 0.5 mL·min^{-1}. Detection was performed using a three-detectors static light-scattering apparatus (MiniDAWN TrEOS; Wyatt Technology) and protein concentration was determined with an online refractometer (Optilab rEX; Wyatt Technology). Molecular weight calculations were performed with the ASTRA V5.3 software (Wyatt Technology), using a *dn/dc* value of 0.183 mL·g^{-1}. MALLS calibration was checked with BSA (2 mg·mL^{-1}; Pierce). Tubulin elutes at 9.1 mL. In presence of D1, the peak of the complex is shifted to a lower retention volume (8.9 mL), indicating the formation of the complex. The derived masses from the static light-scattering data are 98.5 ± 1.3 and 106.5 ± 1.7 kDa for tubulin (Mw_{theo} = 100 kDa; Mw_{theo} is the molecular weight derived from the sequence) and the tubulin–D1 complex (Mw_{theo} = 118 kDa) respectively, consistent with a 1:1 stoichiometry.

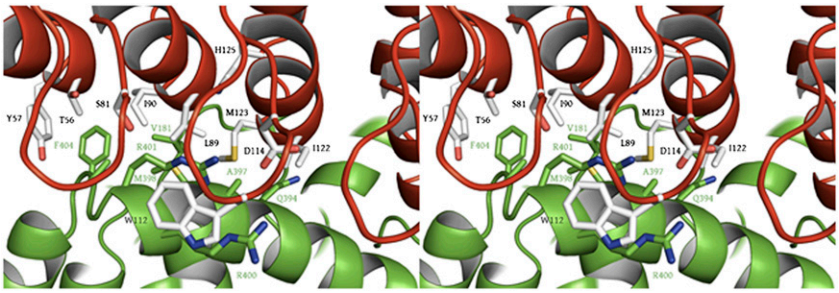

Fig. S2. Stereoview of the interface between D1 and tubulin in Tub-D1. This view is as in Fig. 2*C*. Tubulin is in green and D1 in red. Residues shown in white and labeled in black correspond to the eight randomized positions of the sequence in the library from which D1 was selected.

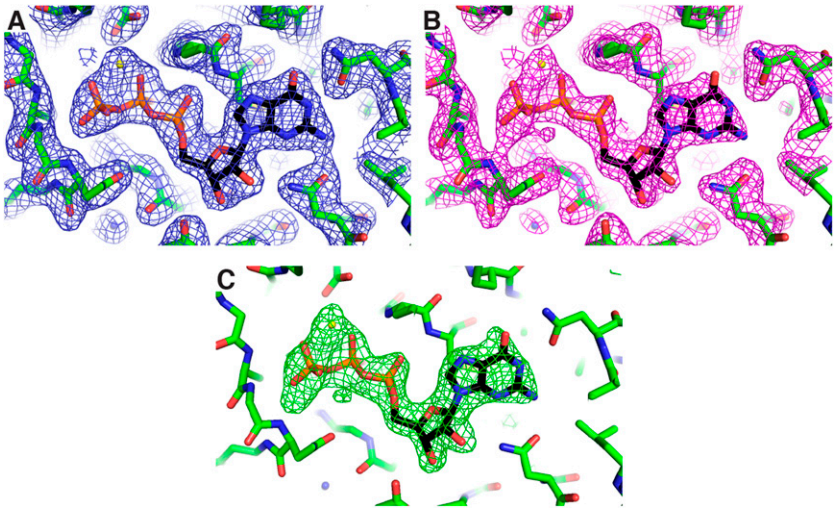

Fig. S3. The tubulin exchangeable nucleotide-binding site is occupied by GTP. Electron density is presented together with the refined atomic model in which tubulin carbons are in green, GTP carbons are black, phosphorus atoms are in orange, and Mg^{2+} is in yellow. (*A*) Section of the $2F_{obs} - F_{calc}$ electron density map contoured at the 1σ level. (*B*) Section of an OMIT $2F_{obs} - F_{calc}$ electron density map contoured at the 1σ level. GTP and Mg^{2+} in the two β-tubulin chains in the asymmetric unit have been omitted from the model, which was refined (three cycles, maximum-likelihood refinement) before structure factor calculation. (*C*) Section of an OMIT $F_{obs} - F_{calc}$ electron density map contoured at the 3σ level; structure factors were calculated as in *B*.

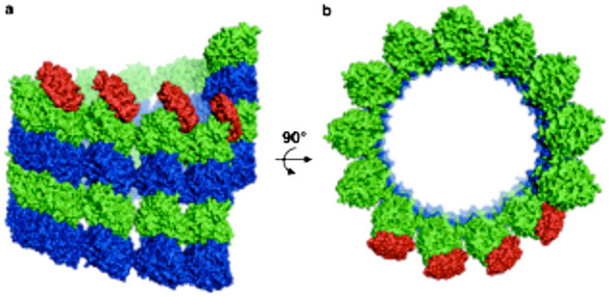

Fig. S4. Model of D1 bound to the (+) end of a 13-protofilament microtubule. This model was obtained by superposing β-tubulin in tubulin–D1 to β-tubulin in the atomic model of a microtubule (PDB ID 2XRP). D1 is in red; α- and β-tubulin are in blue and green, respectively. (*A*) View perpendicular to the microtubule axis. (*B*) View along the microtubule axis.

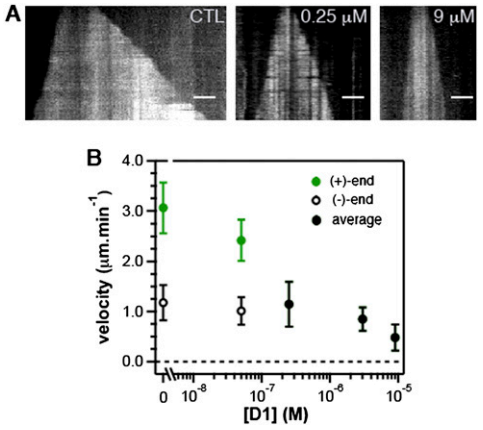

Fig. S5. Microtubule growth inhibition by D1 as observed by TIRF microscopy. (*A*) Representative kymographs of a growing microtubule in the absence of DARPin (control) and in 0.25 μM and 9 μM D1. The total duration of each kymograph is 279 s. (Scale bars, 3 μm.) (*B*) Growth velocity of microtubule (+) and (–) ends in the presence of 20 μM tubulin as a function of increasing D1 concentrations. Growth at (+) and (–) ends could not be distinguished at D1 concentrations of 0.25 μM and higher and average values are given here.

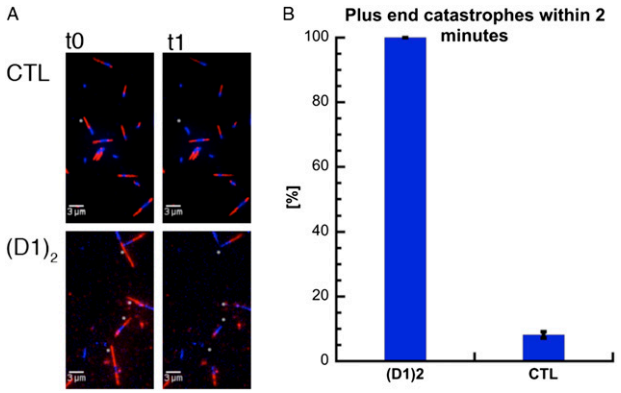

Fig. S6. Percentage of preformed microtubule (+) ends that did undergo a catastrophe within 2 min after buffer exchange. (*A*) Cy5 tubulin (15 μM) (red) was polymerized from GMPCPP-stabilized Alexa568-labeled microtubule seeds (blue) for 90 s, at which point the free Cy5 tubulin was washed out and replaced by 15 μM unlabeled tubulin, 65 nM GFP-Clip170$_{MTB}$, and 500 nM $(D1)_2$ or its storage buffer (CTL) (*Methods*). We counted the Cy5-labeled plus ends at t0 (start of imaging, ∼30 s after buffer exchange) and t1 (90 s after time-lapse movies were started); this quantification is shown in *B*. The identity of each end (plus or minus) was extracted from kymographs (growth speed) of the corresponding GFP-CLIP170$_{MTB}$ channels (*Methods*). Plus-end segments undergoing catastrophe are marked with asterisks. (*B*) The numbers of prepolymerized (+) sections (labeled with Cy5) were quantified at different time points after solution exchange (50 sections per condition). In the presence of 0.5 μM $(D1)_2$ the number of these sections decreased rapidly, leading to an ∼10-fold reduction after 2 min in comparison with the control without $(D1)_2$.

Table S1. Data collection and refinement statistics

	Tubulin–D1
Data collection*	
Space group	$P2_1$
Cell dimensions	
a, *b*, *c*, Å	104.55, 90.30, 117.27
α, β, γ, °	90.00, 90.16, 90.00
Resolution, Å	39.19–2.22 (2.35–2.22)
R_{sym} or R_{merge}	8.6 (66.7)
$I/\sigma I$	12.4 (2.1)
Completeness, %	96.1 (95.0)
Redundancy	3.0 (3.0)
Refinement	
Resolution, Å	2.22
No. reflections	104,776
R_{work}/R_{free}	0.159/0.194
No. atoms	
Protein	15,555
Ligand/ion	132
Water	345
B-factors	
Protein	41.1
Ligand/ion	33.8
Water	34.6
rms deviations	
Bond lengths, Å	0.01
Bond angles, °	0.804

*Data were collected on a single crystal. Values in parentheses are for highest-resolution shell.

Table S2. Residues at the tubulin-D1 interface

D1*	β-Tubulin†
Arg-23	His-406
Thr-56	Ala-403
Tyr-57	**Phe-404**
Ser-81	Arg-401
Leu-86	Arg-401
Leu-89	Val-181/Ala-397/**Met-398**/Arg-401
Ile-90	Val-181/**Met-398**/Ala-403/**Phe-404**
Asp-110	Arg-401
Trp-112	Arg-400/Arg-401
Asp-114	Arg-401
Leu-119	Ala-397/Arg-401
Ile-122	Glu-393/Gln-394/Ala-397
Met-123	Val-181/Gln-394/**Met-398**
Gly-124	Pro-175
His-125	Val-181
Ile-152	Glu-393
Asn-156	Arg-390/Glu-393
Asn-158	**Lys-176**/Glu-207
Glu-159	Asp-211/Arg-215/
Asp-160	**Lys-176/Tyr-210**/Phe-214/Arg-215

*Underlined residues correspond to D1 randomized position.
†Residue numbering is according to ref. 1; residues in boldface type participate in longitudinal contacts when tubulin is embedded in a microtubule.

1. Löwe J, Li H, Downing KH, Nogales E (2001) Refined structure of αβ-tubulin at 3.5 Å resolution. *J Mol Biol* 313:1045–1057.